

Supplementary Information for

A Spectroscopic Ruler for Measuring Active Site Distortions based on Raman Optical Activity of a Hydrogen Out-of-Plane Vibration

Shojiro Haraguchi, Takahito Shingae, Tomotsumi Fujisawa, Noritaka Kasai, Masato Kumauchi, Takeshi Hanamoto, Wouter D. Hoff, and Masashi Unno

Masashi Unno

Email: unno@cc.saga-u.ac.jp

This PDF file includes:

Supplementary text

Figs. S1 to S8

Tables S1 to S5

References for SI reference citations

Supplemental Data

Table S1. Structural parameters (dihedral angles in degree) of the crystal structures and active site model for PYP

PDB/ model	Res. ^a	C3–C4 –C7–C8	C4–C7 –C8–C9	C7–C8 –C9–O2	C1–C2 –C3–H3	C3–C4 –C7–H7	H7–C7 –C8–H8	Ref.
2PHY	1.4	-2.4	173.6	-22.7	-	-	-	(1)
1D7E	1.39	5.9	165.8	-12.6	-	-	-	(2)
1NWZ	0.82	-2.4	165.1	-11.5	-	-	-	(3)
1OT9	1.0	-7.5	167.6	-11.6	-	-	-	(4)
1OTB	1.1	-8.3	169.2	-8.3	-	-	-	(4)
2D01	1.34	-4.6	172.3	-18.4	-	-	-	(5)
2QWS	2.5	-6.5	171.8	-3.9	-	-	-	(6)
2QJ7	1.05	-0.4	176.9	-2.6	-	-	-	(7)
2ZOI	1.5	-4.7	168.2	-10.0	-169.4	-179.8	-172.5	(8)
model 1		-10.0	170.0	-10.0	-170.0	-179.8	-170.0	

^aResolution in Å.

Resonance Raman spectra of the pB state for PYP. We measured the resonance Raman spectra of the pB state for PYP with 325 nm excitation, and the result is shown in Fig. S1. The observed spectra were simulated by the DFT calculations using protonated *cis*-form of *p*-coumaric acid methyl thiol ester as a model (models A and B, Fig. S2). The results confirmed our previous assignment of the Raman bands for pB.

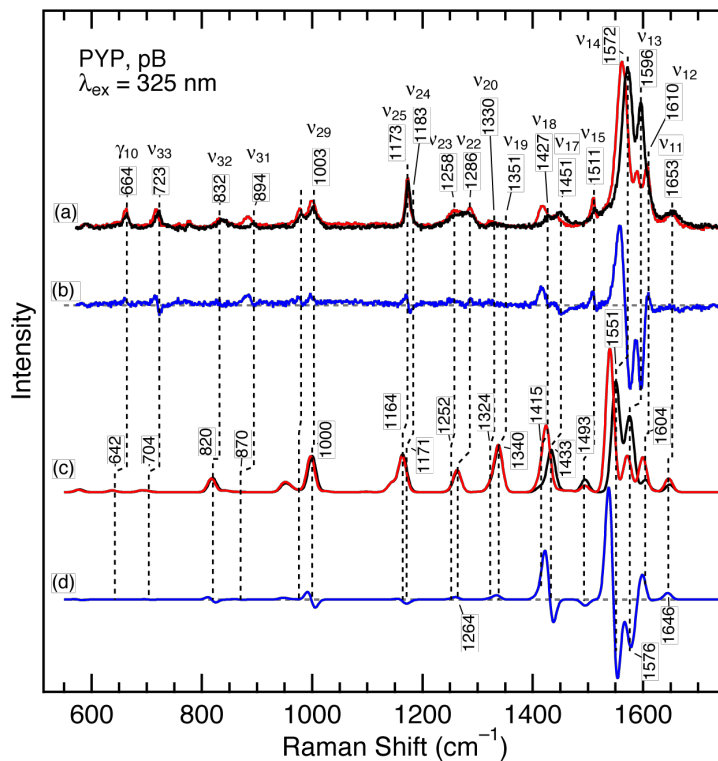


Fig. S1. Observed and calculated Raman spectra of the pB state of PYP. The spectra for the unlabeled (black) and $^{13}\text{C}_8$ -labeled (red) samples as well as the ^{13}C - ^{12}C difference spectra (blue) are displayed. The calculated spectrum is an average of two spectra based on models 2A and 2B. Gaussian band shapes with a 10 cm^{-1} width were used.

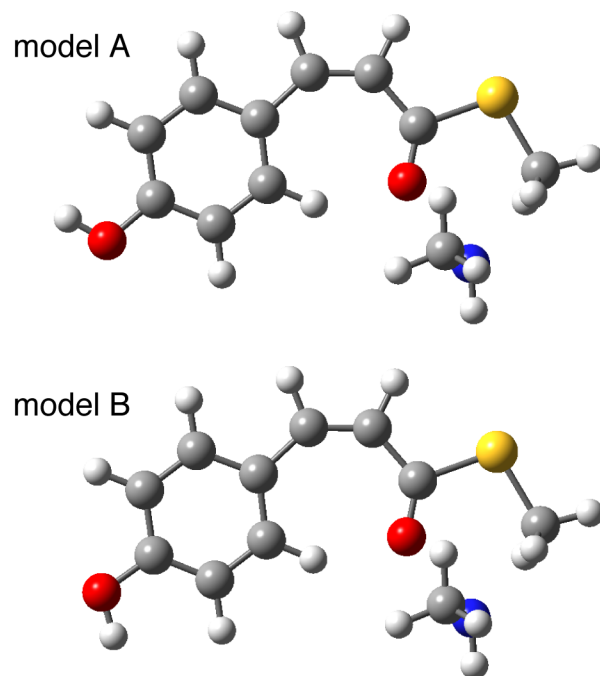


Fig. S2. Optimized geometries of two models for the pB state of PYP. Black, blue, red, and yellow represent carbon, nitrogen, oxygen, and sulfur atoms, respectively.

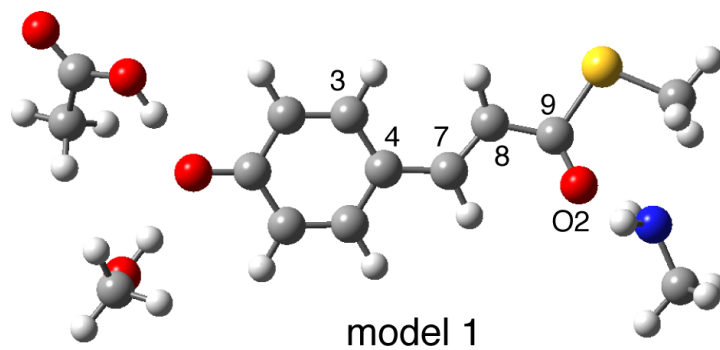


Fig. S3. Optimized geometry (model 1) for the pG state of PYP. Black, blue, red, and yellow represent carbon, nitrogen, oxygen, and sulfur atoms, respectively. All quantum chemical calculations were performed using Gaussian09 (9).

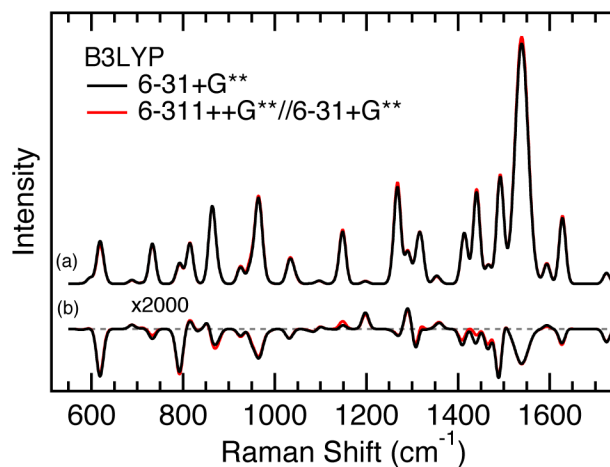


Fig. S4. Calculated Raman and ROA spectra of the active site model of PYP (model 1). The spectra drawn in black were computed by a B3LYP/6-31+G** level of theory. For the spectra drawn in red, Raman and ROA intensities were calculated by B3LYP/6-311++G**, while B3LYP/6-31+G** was used for the geometry optimization and force field calculation.

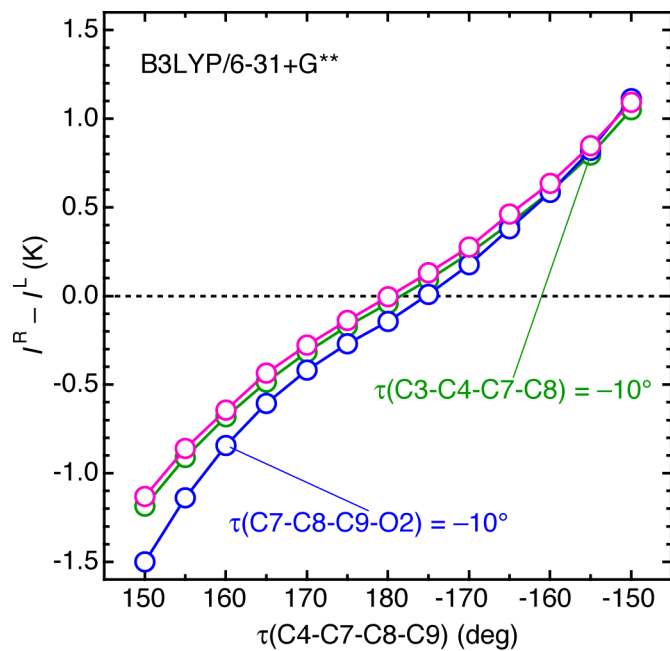


Fig. S5. ROA intensities for γ_8 as a function of the dihedral twists about the C7=C8 bond $\tau(\text{C4-C7-C8-C9})$ for the chromophore model of PYP.

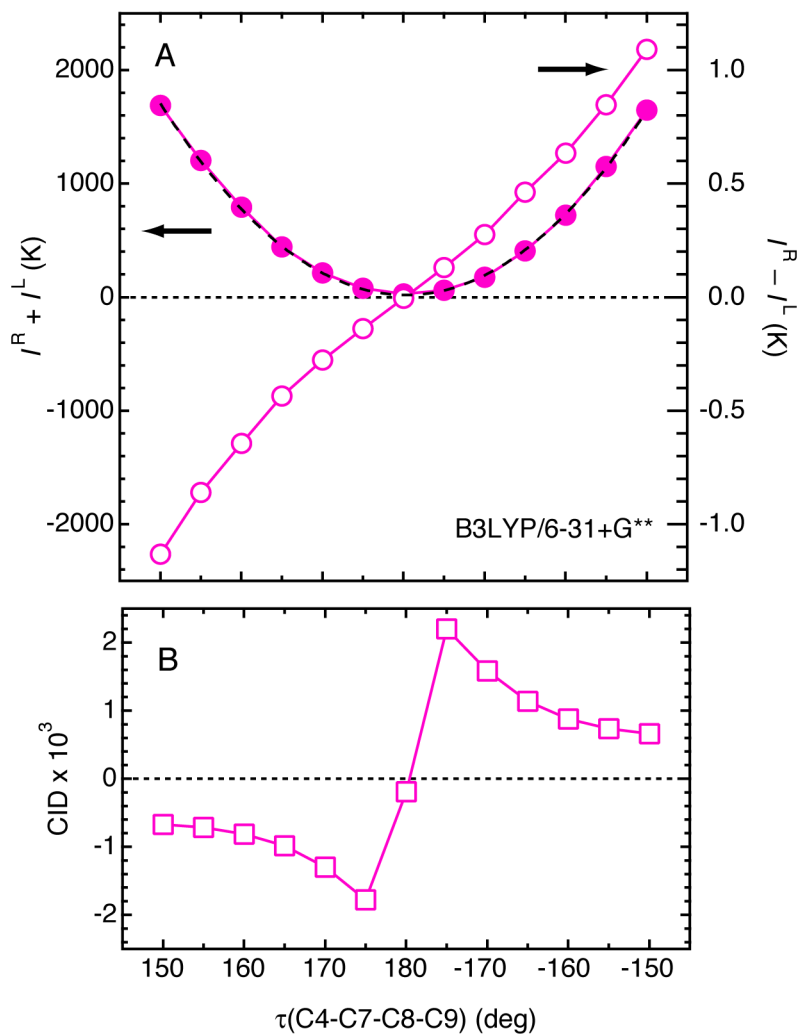


Fig. S6. Raman and ROA intensities and circular intensity difference (CID) as a function of the dihedral twists about the C7=C8 bond for the chromophore model of PYP. Raman intensities are fitted with a parabolic curve. The fitted curve is shown as the dashed line in panel A.

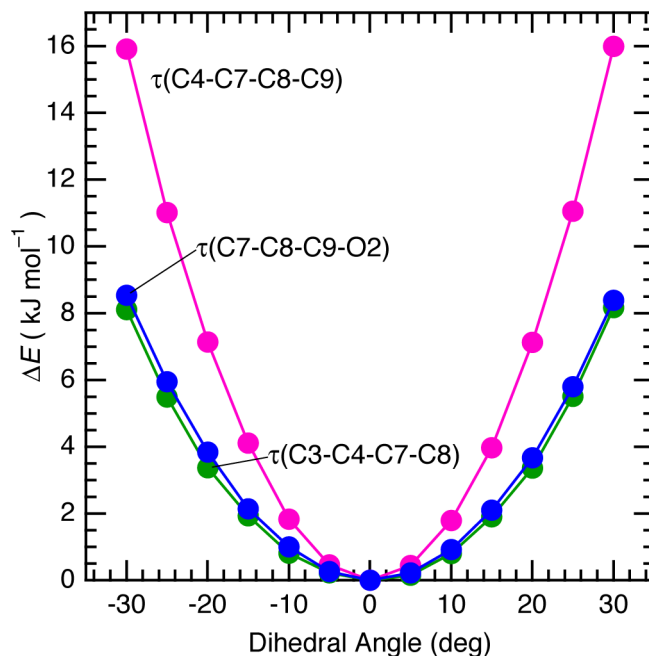


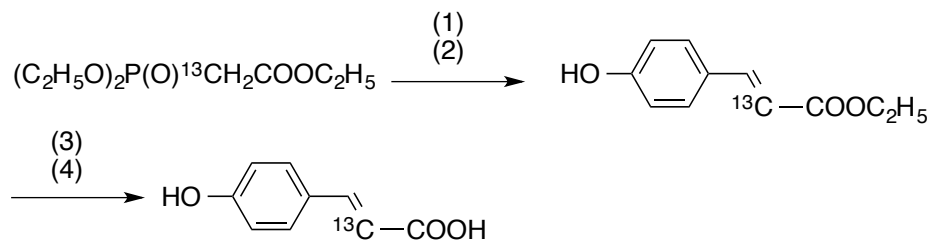
Fig. S7. Changes in energy associated with the dihedral twists of $\tau(\text{C3-C4-C7-C8})$, $\tau(\text{C4-C7-C8-C9})$, and $\tau(\text{C7-C8-C9-O2})$ for the chromophore model of PYP. Energies were calculated by B3LYP/6-31+G**. For $\tau(\text{C4-C7-C8-C9})$, the horizontal axis stands for differences in the dihedral angle from a planar geometry.

Supplemental Experimental Section

Preparation of $^{13}\text{C}8$ -Labeled *p*-Coumaric acid

$^{13}\text{C}8$ -labeled *p*-coumaric acid (*p*CA) was prepared according to the method described previously (10) with its minor modification (Schemes 1).

Scheme 1. Preparation of *p*-Coumaric[8- $^{13}\text{C}_1$] Acid



- (1) Toluene, sodium hydride in mineral oil 60 % at RT under Ar, 30 min
- (2) 4-Hydroxybenzaldehyde in ether at 60°C under Ar, 4 hr, NH_4Cl aq
- (3) KOH aq (1 mol/L), 35°C for 12 hr, redissolution
- (4) HCl aq (6 mol/L), precipitate

The ^{13}C -labeled reagent, triethylphosphonoacetate (1- ^{13}C , 99%) (Cambridge Isotope Laboratory) was used and was commercially available. Under an argon atmosphere, 4-hydroxybenzaldehyde was treated with phosphonate anion, which was generated from triethylphosphonoacetate at room temperature. After 4 h stirring, ethyl 4-hydroxycinnamate was obtained and then hydrolyzed in 1 mol/L potassium hydroxide solution. After usual workup and purification, colorless $^{13}\text{C}8$ -labeled *p*-coumaric acid (4-hydroxycinnamic acid) was obtained. The purity was checked with GCMS and ^1H NMR spectroscopy.

Theoretical Considerations of Raman and ROA Intensities

1. Raman Intensity

In this study, we have performed systematic DFT calculations and showed that the ROA intensities are roughly proportional to the dihedral twists of the chromophore. On the contrary, the Raman intensities exhibit a non-linear dependence on the dihedral twist (Fig. 3, Fig. S6). In order to explain these differences, we have made theoretical considerations of Raman and ROA intensities. Using far-from-resonance (FFR) approximation, the Raman transition polarizability from vibrational levels 0 to 1 of the ground electronic state for a polyene chain, which adopts a planar geometry, is given by:(11)

$$\left(\alpha_{\alpha\beta}^0\right)_{1,0} = \langle\phi_1|\frac{1}{\hbar}\sum_e\left[\frac{\langle g|\hat{\mu}_\alpha|e\rangle\langle e|\hat{\mu}_\beta|g\rangle}{\omega_{eg}-\omega_0}+\frac{\langle g|\hat{\mu}_\beta|e\rangle\langle e|\hat{\mu}_\alpha|g\rangle}{\omega_{eg}+\omega_0}\right]|\phi_0\rangle$$

where ω_{eg} represents the frequency (energy) difference between the initial state g and the intermediate state e . $\hat{\mu}_\alpha$ is a electric dipole operator.

$$\hat{\mu}_\alpha = e\hat{r}_\alpha$$

The summation is over all excited states of the molecule. ϕ_0 and ϕ_1 are the nuclear wavefunctions responsible for describing the vibrational states 0 and 1 in the electronic state g of the molecule, respectively. Greek subscripts represent the Cartesian components, i.e., x , y , and z . The elements of the Raman polarizability tensor depend on the orientation of the molecule with respect to an xyz -reference frame. However, we can take combinations of tensor elements that are invariant to changes in the orientation of the molecule in the reference frame. These combinations are called invariants. In this section we will consider how Raman and ROA invariants for a hydrogen out-of-plane (HOOP) mode are perturbed, when the polyene chain experiences the out-of-plane distortion. First, we assume that an internal coordinate associated with the distortion is represented by $Q_\theta \cdot \theta$, when the polyene chain is twisted along the coordinate Q_θ , by a dihedral angle of θ . Here, the distortion coordinate Q_θ is generally expressed by the linear combination of the vibrational normal mode Q_n as

$$Q_\theta = \sum_{n=1}^{3N-6} a_n Q_n. \quad (1)$$

Then, we write the nuclear coordinate dependence of the electronic wavefunctions as a quantum mechanical perturbation expression, which is analogous to the Herzberg–Teller expansion as follows:

$$|g\rangle = |g\rangle^0 + \sum_{n=1}^{3N-6} a_n \frac{\partial |g\rangle}{\partial Q_n} Q_n \cdot \theta \quad (2a)$$

$$|e\rangle = |e\rangle^0 + \sum_{n=1}^{3N-6} a_n \frac{\partial |e\rangle}{\partial Q_n} Q_n \cdot \theta \quad (2b)$$

By contrast, the nuclear wavefunctions depend only on second order in θ , and there is no first order term. The potential energy difference ΔV can be expressed using force constant k as

$$\Delta V = \frac{1}{2} k (Q_\theta \cdot \theta)^2 \quad (3)$$

Because the nuclear wavefunction is written by the following perturbation expression

$$\phi_0^\theta = \phi_0^0 + \sum_{s \neq 0} \frac{\langle \phi_s^0 | \Delta V | \phi_0^0 \rangle}{E_0 - E_s} \phi_s^0 + \dots, \quad (4)$$

there is only second order term in θ . On the basis of these considerations, we can write the Raman transition polarizability to first order in θ by

$$(\alpha_{\alpha\beta})_{1,0} = (\alpha_{\alpha\beta}^0)_{1,0} + \sum_{n=1}^{3N-6} a_n \left(\frac{\partial \alpha_{\alpha\beta}}{\partial Q_n} \right)_{Q_n=0} \langle \phi_1 | Q_n | \phi_0 \rangle \theta \equiv (\alpha_{\alpha\beta}^0)_{1,0} + (\Delta \alpha_{\alpha\beta})_{1,0} \theta \quad (5)$$

where

$$\left(\frac{\partial \alpha_{\alpha\beta}}{\partial Q_n} \right)_{Q_n=0} = \frac{\partial}{\partial Q_n} \left[\frac{\langle g | \hat{\mu}_\alpha | e \rangle \langle e | \hat{\mu}_\beta | g \rangle}{\omega_{eg} - \omega_0} + \frac{\langle g | \hat{\mu}_\beta | e \rangle \langle e | \hat{\mu}_\alpha | g \rangle}{\omega_{eg} + \omega_0} \right]_{Q_n=0} \quad (6)$$

Equation (5) indicates that the distortion-induced change in the Raman polarizability of a given normal mode Q_n is proportional to how much the normal mode is included in the distortional coordinate (i.e., a_n) and the Raman polarizability before the structural perturbation (i.e., $(\partial \alpha_{\alpha\beta} / \partial Q_n)_{Q_n=0}$). Using Equation (5), the Raman scattering invariant α^2 is given as follow:

$$\alpha^2 = \frac{1}{9} \sum_{\alpha,\beta} \alpha_{\alpha\alpha} \alpha_{\beta\beta} = \frac{1}{9} \sum_{\alpha,\beta} (\alpha_{\alpha\alpha}^0 + \Delta \alpha_{\alpha\alpha} \cdot \theta) \cdot (\alpha_{\beta\beta}^0 + \Delta \alpha_{\beta\beta} \cdot \theta) \quad (7)$$

For a representative HOOP mode with A_u symmetry in Fig. S8 (cf. Table S2), $(\alpha_{\alpha\alpha}^0)_{1,0}$ is zero at $\theta = 0$ because the symmetry of the Raman polarizability tensor is A_g or B_g , while that of the vibrational mode is A_u . In this case, we can write the invariant as follows:

$$\alpha^2 = \frac{1}{9} \sum_{\alpha,\beta} \Delta\alpha_{\alpha\alpha} \cdot \Delta\alpha_{\beta\beta} \cdot \theta^2 \quad (8)$$

Analogously, the Raman scattering invariant $\beta(\alpha)^2$ is given by Equation (9).

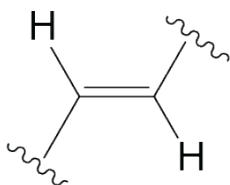
$$\beta(\alpha)^2 = \frac{1}{2} \sum_{\alpha,\beta} (3\alpha_{\alpha\beta}\alpha_{\alpha\beta} - \alpha_{\alpha\alpha}\alpha_{\beta\beta}) = \frac{1}{2} \sum_{\alpha,\beta} (3 \cdot \Delta\alpha_{\alpha\beta} \cdot \Delta\alpha_{\alpha\beta} - \Delta\alpha_{\alpha\alpha} \cdot \Delta\alpha_{\beta\beta}) \cdot \theta^2 \quad (9)$$

Equations (8) and (9) indicate that the dihedral twist θ makes only a second-order contribution to the Raman invariant α^2 and $\beta(\alpha)^2$. We note that the symmetry-based argument is less applicable as the symmetry of the vibrational mode is worse. However, for the HOOP modes, which typically show the small intensities when the molecule is planar, the same argument with A_u -type HOOP mode still holds.

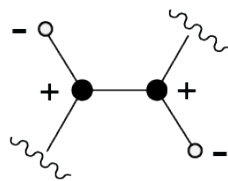
Generally, if we start from the achiral conformation (e.g. planar polyene) and distort it by changing the dihedral angle with $+\theta$ and $-\theta$, we obtain two enantiomers that have the same Raman intensities; the Raman intensity is even function of θ . Therefore, the quadratic term is expected to be a major contributor to the θ dependence.

Table S2. Character table of C_{2h} for the ethylenic group

C_{2h}	E	C_2	i	σ_h		
A_g	1	1	1	1	R_z	x^2, y^2, z^2, xy
B_g	1	-1	1	-1	R_x, R_y	xz, yz
A_u	1	1	-1	-1	z	
B_u	1	-1	-1	1	x, y	



Ethylenic group



A_u -type HOOP vibration

Fig. S8. Illustration of A_u -type HOOP (hydrogen-out-of-plane) mode.

2. ROA Intensity

There are many forms of ROA. In this study, we used incident circular polarization (ICP) ROA, in which the laser radiation is switched between right and left circularly polarized states, unpolarized Raman scattered radiation is detected. The theoretical expression for back-scattering geometry is given by: (11)

$$ICP_U(180^\circ): \quad I_U^R(180^\circ) - I_U^L(180^\circ) = \frac{8K}{c} [12\beta(G')^2 + 4\beta(A)^2] \quad (10)$$

where K is a constant, c is the speed of light, and $\beta(G')^2$ and $\beta(A)^2$ are ROA invariants that will be defined later. Note that if these expressions are compared with those for unpolarized backscattering scattered circular polarization (SCP) ROA, one can see that, in the FFR approximation, these two experiments give exactly the same results. To evaluate these invariants, we first consider magnetic dipole optical activity tensor $G_{\alpha\beta}$ for a planar geometry.

$$(G_{\alpha\beta}^0)_{1,0} = \langle \phi_1 | \frac{1}{\hbar} \sum_e \left[\frac{\langle g | \hat{\mu}_\alpha | e \rangle \langle e | \hat{m}_\beta | g \rangle}{\omega_{eg} - \omega_0} + \frac{\langle g | \hat{m}_\beta | e \rangle \langle e | \hat{\mu}_\alpha | g \rangle}{\omega_{eg} + \omega_0} \right] | \phi_0 \rangle \quad (11)$$

where \hat{m}_α is a magnetic dipole operator.

$$\hat{m}_\alpha = \frac{e}{2m} (\hat{\mathbf{r}} \times \hat{\mathbf{p}})_\alpha \quad (12)$$

According to Equation (11), we derive

$$(G_{\alpha\beta})_{1,0} = (G_{\alpha\beta}^0)_{1,0} + \sum_{n=1}^{3N-6} a_n \left(\frac{\partial G_{\alpha\beta}}{\partial Q_n} \right)_{Q_n=0} \langle \phi_1 | Q_n | \phi_0 \rangle \theta \equiv (G_{\alpha\beta}^0)_{1,0} + (\Delta G_{\alpha\beta})_{1,0} \theta \quad (13)$$

where

$$\left(\frac{\partial G_{\alpha\beta}}{\partial Q_n} \right)_{Q_n=0} = \frac{\partial}{\partial Q_n} \left[\frac{\langle g | \hat{\mu}_\alpha | e \rangle \langle e | \hat{m}_\beta | g \rangle}{\omega_{eg} - \omega_0} + \frac{\langle g | \hat{m}_\beta | e \rangle \langle e | \hat{\mu}_\alpha | g \rangle}{\omega_{eg} + \omega_0} \right]_{Q_n=0} \quad (14)$$

Next we consider electric quadrupole optical activity tensor $A_{\alpha,\beta\gamma}$ for a planar geometry.

$$(A_{\alpha,\beta\gamma}^0)_{1,0} = \langle \phi_1 | \frac{1}{\hbar} \sum_e \left[\frac{\langle g | \hat{\mu}_\alpha | e \rangle \langle e | \hat{\Theta}_{\beta\gamma} | g \rangle}{\omega_{eg} - \omega_0} + \frac{\langle g | \hat{\Theta}_{\beta\gamma} | e \rangle \langle e | \hat{\mu}_\alpha | g \rangle}{\omega_{eg} + \omega_0} \right] | \phi_0 \rangle \quad (15)$$

where $\hat{\Theta}_{\beta\gamma}^0$ is an electric quadrupole operator.

$$\hat{\Theta}_{\beta\gamma}^0 = \frac{e}{2} (3r_\beta r_\gamma - r^2 \delta_{\beta\gamma}) \quad (16)$$

According to Equation (15), electric quadrupole optical activity tensor for a distorted polyene chain is given by:

$$(A_{\alpha,\beta\gamma})_{1,0} = (A_{\alpha,\beta\gamma}^0)_{1,0} + \sum_{n=1}^{3N-6} a_n \left(\frac{\partial A_{\alpha,\beta\gamma}}{\partial Q_n} \right)_{Q_n=0} \langle \phi_1 | Q_n | \phi_0 \rangle \theta \equiv (A_{\alpha,\beta\gamma}^0)_{1,0} + (\Delta A_{\alpha,\beta\gamma})_{1,0} \theta \quad (17)$$

where

$$\left(\frac{\partial A_{\alpha,\beta\gamma}}{\partial Q_n} \right)_{Q_n=0} = \frac{\partial}{\partial Q_n} \left[\frac{\langle g | \hat{\mu}_\alpha | e \rangle \langle e | \hat{\Theta}_{\beta\gamma} | g \rangle}{\omega_{eg} - \omega_0} + \frac{\langle g | \hat{\mu}_\gamma | e \rangle \langle e | \hat{\Theta}_{\alpha\beta} | g \rangle}{\omega_{eg} + \omega_0} \right]_{Q_n=0} \quad (18)$$

As described above, two ROA invariants, $\beta(G')^2$ and $\beta(A)^2$, contribute to the backscattering ROA under FFR approximation. In the other forms of ROA such as right-angle scattering, an invariant αG also contributes to the ROA intensity. This invariant can be expressed using Equations (5) and (14) as follows:

$$\alpha G = \frac{1}{9} \sum_{\alpha,\beta} \alpha_{\alpha\alpha} G_{\beta\beta} = \frac{1}{9} \sum_{\alpha,\beta} (\alpha_{\alpha\alpha}^0 + \Delta\alpha_{\alpha\alpha} \cdot \theta) \cdot (G_{\beta\beta}^0 + \Delta G_{\beta\beta} \cdot \theta) \quad (19)$$

For A_u type HOOP mode, for instance, $(\alpha_{\alpha\alpha}^0)_{1,0}$ is zero because the symmetry of the Raman polarizability tensor is not A_u but A_g or B_g . By contrast, since the elements of $\langle g | \hat{\mu}_\alpha | e \rangle \langle e | \hat{\mu}_\alpha | g \rangle$ exhibit A_u symmetry, $(G_{\alpha\alpha}^0)_{1,0}$ is non-zero (cf. Table S3). We therefore obtain the following expression.

$$\alpha G = \frac{1}{9} \sum_{\alpha,\beta} (\Delta\alpha_{\alpha\alpha} \cdot G_{\beta\beta}^0 \cdot \theta + \Delta\alpha_{\alpha\alpha} \Delta G_{\beta\beta} \cdot \theta^2 + \dots) \quad (20)$$

In a similar way, the invariant $\beta(G)^2$ can be given by:

$$\begin{aligned} \beta(G)^2 &= \frac{1}{2} \sum_{\alpha,\beta} (3\alpha_{\alpha\beta} G_{\alpha\beta} - \alpha_{\alpha\alpha} G_{\beta\beta}) \\ &= \frac{1}{2} \sum_{\alpha,\beta} \left[(3\Delta\alpha_{\alpha\beta} \cdot G_{\alpha\beta}^0 - \Delta\alpha_{\alpha\alpha} \cdot G_{\beta\beta}^0) \theta + (3\Delta\alpha_{\alpha\beta} \cdot \Delta G_{\alpha\alpha} - \Delta\alpha_{\alpha\alpha} \cdot \Delta G_{\beta\beta}) \theta^2 + \dots \right] \end{aligned} \quad (21)$$

Next we consider ROA invariant $\beta(A)^2$, which is related to electric quadrupole optical activity tensor, as follows:

$$\begin{aligned} \beta(A)^2 &= \frac{1}{2} \omega_0 \sum_{\alpha,\beta,\gamma,\delta} \alpha_{\alpha\beta} \epsilon_{\alpha\gamma\delta} A_{\gamma,\delta\beta} \\ &= \frac{1}{2} \omega_0 \sum_{\alpha,\beta,\gamma,\delta} (\alpha_{\alpha\beta}^0 + \Delta\alpha_{\alpha\beta} \cdot \theta) \epsilon_{\alpha\gamma\delta} (A_{\gamma,\delta\beta}^0 + \Delta A_{\gamma,\delta\beta} \cdot \theta) \end{aligned} \quad (22)$$

In this equation, $\epsilon_{\alpha\gamma\delta}$ is the alternating tensor that equals +1 for even permutations of x , y , and z and -1 for their odd permutation. For A_u type HOOP mode, $(\alpha_{\alpha\beta}^0)_{1,0}$ is zero as mentioned above, whereas $\langle g | \hat{\mu}_\gamma | e \rangle \langle e | \hat{\Theta}_{\delta\beta} | g \rangle$ shows A_u symmetry (cf. Table S4), so that $(A_{\gamma,\delta\beta}^0)_{1,0}$ is non-zero. Thus $\beta(A)^2$ depends on the dihedral twist θ as described below:

$$\beta(A)^2 = \frac{1}{2} \omega_0 \sum_{\alpha, \beta, \gamma, \delta} \left[(\Delta\alpha_{\alpha\beta} \cdot \varepsilon_{\alpha\gamma\delta} A_{\gamma, \delta\beta}^0) \theta + (\Delta\alpha_{\alpha\beta} \cdot \varepsilon_{\alpha\gamma\delta} \cdot \Delta A_{\gamma, \delta\beta}) \theta^2 + \dots \right] \quad (23)$$

As given in Equations (20), (21) and (23), the distortion-induced changes in the ROA invariants are proportional to the change in Raman polarizability under distorted conformation, $\Delta\alpha_{\alpha\beta}$ (in Equation (5)). Besides, the ROA invariants show a first-order dependence on the dihedral twist θ . This is distinctly different from the Raman invariants, which exhibit only a second-order dependence on θ . The difference between the Raman and ROA intensities is consistent with the results of the DFT calculations shown in Fig. S6. We note that the argument using A_u -type HOOP mode is less applicable as the symmetry of the vibrational mode is worse. However, $(\alpha_{\alpha\beta}^0)_{1,0}$ of HOOP modes is typically small when the molecule is planar and $(G_{\alpha\beta}^0)_{1,0}$ (and also $(A_{\gamma, \delta\beta}^0)_{1,0}$) are expected to be non-zero because the nuclear displacement along the HOOP mode makes the polyene chain chiral. The same argument with A_u -type HOOP mode, therefore, can hold for other HOOP modes.

If we consider a case that distorts an achiral conformation by changing the dihedral angle with $+\theta$ and $-\theta$, we obtain two enantiomers whose ROA intensities have the opposite signs but the same magnitudes, i.e., the ROA intensity is odd function of θ . Thus, in the case of ROA, the linear term is expected to be a major contributor to the θ dependence.

Table S3. Irreducible representation of G_{ij} elements for A_u HOOP mode, which is obtained from the direct product of i ($= x, y,$ and z) and R_j ($= R_x, R_y,$ and $R_z,$ cf. Table S2)

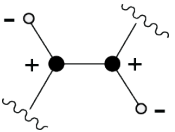
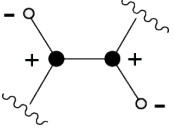
 G_{ij} element	E	C_2	i	σ_h	irreducible representation
G_{xx}	1	1	-1	-1	A_u
G_{yy}	1	1	-1	-1	A_u
G_{zz}	1	1	-1	-1	A_u
G_{xy}	1	1	-1	-1	A_u
G_{xz}	1	-1	-1	1	B_u
G_{yx}	1	1	-1	-1	A_u
G_{yz}	1	-1	-1	1	B_u
G_{zx}	1	-1	-1	1	B_u
G_{zy}	1	-1	-1	1	B_u

Table S4. Irreducible representation of G_{ij} elements for A_u HOOP mode, which is obtained from the direct product of i ($=x, y,$ and z) and ij ($=xy, yx,$ and zx , cf. Table S2)

 A_{ijk} element	E	C_2	i	σ_h	irreducible representation
A_{xyz}	1	1	-1	-1	A_u
A_{yzx}	1	1	-1	-1	A_u
A_{zxy}	1	1	-1	-1	A_u
A_{yyz}	1	1	-1	-1	A_u
A_{zyy}	1	1	-1	-1	A_u
A_{zxx}	1	1	-1	-1	A_u
A_{xxz}	1	1	-1	-1	A_u
A_{yzz}	1	-1	-1	1	B_u
A_{zzy}	1	-1	-1	1	B_u
A_{xxy}	1	-1	-1	1	B_u
A_{yxx}	1	-1	-1	1	B_u
A_{zzx}	1	-1	-1	1	B_u
A_{xzz}	1	-1	-1	1	B_u
A_{xyy}	1	-1	-1	1	B_u
A_{yyx}	1	-1	-1	1	B_u

3. Estimation of the Distortion-Induced Raman and ROA Intensities

Based on the above-mentioned theoretical considerations, we estimated the relative values of distortion-induced Raman invariants α^2 and $\beta(\alpha)^2$ for HOOP modes, γ_2 , γ_8 , and γ_{10} from the DFT calculations (B3LYP/6-31+G**). According to the calculated values in Table S5, the HOOP modes dominantly gain the Raman intensities from the invariant $\beta(\alpha)^2$. After confirming the quadric dependence of their Raman intensities on $\tau(\text{C4-C7-C8-C9})$, the changes in the Raman invariant, $\Delta\beta^2 = \frac{1}{2} \sum_{\alpha,\beta} (3 \cdot \Delta\alpha_{\alpha\beta} \cdot \Delta\alpha_{\alpha\beta} - \Delta\alpha_{\alpha\alpha} \cdot \Delta\alpha_{\beta\beta})$, due to the structural distortion about $\tau(\text{C4-C7-C8-C9})$ is estimated. The $\Delta\beta^2$ is derived from Equation (5) and (9) as the product of $\beta(\alpha)^2$ at $\tau(\text{C4-C7-C8-C9}) = 0$ and the square of the HOOP mode contributions $a(\gamma_2, \gamma_8, \text{ or } \gamma_{10})$ in the structural distortion with $\tau(\text{C4-C7-C8-C9})$. When the invariant α^2 is small in comparison to $\beta(\alpha)^2$, the relative amplitude of $\Sigma\Delta\alpha_{ij}$ that is proportional to the back-scattered ROA intensity is obtained as the square root of $\Delta\beta^2$. The γ_8 mode has the largest $\Sigma\Delta\alpha_{ij}$.

Table S5. Raman invariants α^2 and $\beta(\alpha)^2$ for HOOP modes γ_2 , γ_8 , and γ_{10} from the DFT calculation (B3LYP/6-31+G) at the dihedral angle $\tau(\text{C4-C7-C8-C9}) = 0$.^a**

	γ_2	γ_8	γ_{10}
$a(\gamma_2, \gamma_8, \text{ or } \gamma_{10})$	1 %	1 %	3 %
α^2	0.0004	0.0002	0.0026
$\beta(\alpha)^2$	0.123	1.024	0.0188
$\Delta\beta^2$	$\sim 0.123 \times 1^2 = 0.123$	$\sim 1.024 \times 1^2 = 1.024$	$\sim 0.0188 \times 3^2 = 0.0564$
$\Sigma\Delta\alpha_{ij}$	~ 0.3	~ 1	~ 0.2

^a $a(\gamma_2, \gamma_8, \text{ or } \gamma_{10})$ is the estimated HOOP mode contributions in the structural changes with $\tau(\text{C4-C7-C8-C9})$. $\Delta\beta^2$ and $\Sigma\Delta\alpha_{ij}$ are the estimated changes in $\beta(\alpha)^2$ and $\Sigma\alpha_{ij}$ due to the structural perturbation to a change in the dihedral angle $\tau(\text{C4-C7-C8-C9})$.

References

1. Borgstahl, GEO; Williams, DR; Getzoff, ED (1995) 1.4 Å Structure of photoactive yellow protein, a cytosolic photoreceptor: unusual fold, active site, and chromophore. *Biochemistry* 34: 6278–6287.
2. Van Aalten DMF, Joshua-Tor L, Crielaard W, Hellingwerf KJ (2000) Conformational substates in different crystal forms of the photoactive yellow protein—Correlation with theoretical and experimental flexibility. *Protein Sci* 9:64–72.
3. Getzoff ED, Gutwin KN, Genick UK (2003) Anticipatory active-site motions and chromophore distortion prime photoreceptor PYP for light activation. *Nat Struct Mol Biol* 10:663.
4. Anderson S, Crosson S, Moffat K (2004) Short hydrogen bonds in photoactive yellow protein. *Acta Crystallogr D Biol Crystallogr* 60:1008–1016.
5. Shimizu N, Kamikubo H, Yamazaki Y, Imamoto Y, Kataoka M (2006) The crystal structure of the R52Q mutant demonstrates a role for R52 in chromophore pKa regulation in photoactive yellow protein. *Biochemistry* 45:3542–3547.
6. Fisher SZ, et al. (2007) Neutron and X-ray structural studies of short hydrogen bonds in photoactive yellow protein (PYP). *Acta Crystallogr D Biol Crystallogr* 63:1178–1184.
7. Coureux P-D, Fan ZP, Stojanoff V, Genick UK (2008) Picometer-scale conformational heterogeneity separates functional from nonfunctional states of a photoreceptor protein. *Structure* 16:863–872.
8. Yamaguchi S, et al. (2009) Low-barrier hydrogen bond in photoactive yellow protein. *Proc Natl Acad Sci* 106:440–444.
9. Frisch MJ, et al. (2009) *Gaussian 09* (Gaussian, Inc., Wallingford, CT).
10. Wadsworth WS, Emmons WD (1961) The utility of phosphonate carbanions in olefin synthesis. *J Am Chem Soc* 83:1733–1738.
11. Nafie LA (2011) *Vibrational optical activity: Principles and applications* (John Wiley & Sons Ltd., West Sussex)